Electronic Supplementary Material (ESI) for Nanoscale.

Supporting Information

Sequential structural degradation of red perovskite quantum dots and its prevention by introducing iodide at a stable gradient concentration into the core–shell red perovskite quantum dots

Hanleem Lee [a,b,c]*, Cuc Kim Trinh* [a]*, Mo Geun So* [a]*, and Chang-Lyoul Lee* [a,*]

[a]Advanced Photonics Research Institute (APRI), Gwangju Institute of Science and Technology (GIST), Gwangju 61005, Republic of Korea.

[b]Department of Chemistry, Myongji University, 116 Myongji Ro, Yongin, Gyeonggi-do, 17058, Republic of Korea

[c]The Natural Science Research Institute, Myongji University, 116 Myongji Ro, Yongin, Gyeonggi-do 17058, Republic of Korea

[*]Corresponding author: vsepr@gist.ac.kr

This PDF file includes:

Table of Contents

I. Material characterization

Materials: Lead bromide ($PbBr_2$, ≥ 98%), lead iodine (PbI_2, 99%), oleylamine (OAm, 70%), oleic acid (OAc, 90%), 3-aminopropyl-triethoxysilane (APTES, ≥ 98%), octadecane (ODE, 99%), toluene, *n*-hexane, and methyl acetate were purchased from Sigma-Aldrich.

Preparation of pristine perovskite QDs: The cesium oleate solution is firstly prepared. The Cs stearate (0.25 g), OAc (0.5 mL), OAm (0.5 mL) and ODE (8 mL) are added into the 25 mL three-neck round bottom flask. The solution is firstly stirred under vacuum for 10 min and then is heated up to 100 °C for 1 h until the Cs stearate is fully reacted with the OAc/OAm and totally dissolved. The $PbBr_2$ (0.03 g), PbI_2 (0.11 g), OAc (1.5 mL) and OAm (1.3 mL) and ODE (15 mL) are stirred in another 25 mL three-neck round bottom flask under vacuum for 10 min, then the solution is heated up to 100 °C for 30 min. Then, the solution is heated up to 160 °C under N_2 for 10 min. The Cs-oleate (0.7 mL) is swiftly injected into the solution, and after ~5 s, the flask is putted into the ice bath. The product is precipitated by the methyl acetate and then centrifuged at 15,000 rpm for 5 min, and then dispersed in toluene. The precipitate is purified two times. The final precipitate is dispersed in *n*-hexane.

Sample preparation for XPS and XRD anaylsis: The 2 mg/mL perovskite QDs or QD/*x*APTES in *n*-hexane is spin coated at 3krpm (thickness ~15 nm). The samples are dried in vacuum chamber for 30 min to remove solvent and then the XPS and XRD are measured right after drying. Depth-profiling XPS is conducted using Ar plasma etching to prevent the oxidation during the etching process. Depth-profiling XPS of core is estimated at ~18 s Ar plasma etching for pristine perovskite QDs and ~30 s for perovskite/SiO_2 core–shell QDs.

Depth-profiling XPS analysis: PeLEDs with ITO/PEDOT:PSS (50 nm)/perovskite QD/TPBi (30 nm)/Al (150 nm) architectures were fabricated. The Al layer of PeLEDs was firstly peeled off using scotch tape and the TPBi layer was etched with Ar plasma until the Pb component was detected. Depth-profiling XPS experiments for PeLEDs were recorded within 60s Ar plasma etching right after TPBi was removed. We conducted the depth-profiling XPS only at the interface between ETL and single layer of perovskite QDs in PeLEDs to observe the sequential degradation along with cation-defect-assisted ion migration (halide and Cs^+). The Ar plasma etching condition was selected based on the depth-profiling XPS survey using a single layer of perovskite QDs (thickness: ~15 nm, QD size: approximately ~12 ± 2 nm in TEM) on quartz substrate; the Pb component, which related to the existence of perovskite QDs, disappeared within 60 s Ar plasma etching.

In addition, we should emphasize that we are not measuring depth-profiling XPS in the middle of PeLEDs operation, but it is measured right after electrical operation. It is because we want to see the permanent ion migration after electrical operation. When the ion migration happens under the specific electric field, some ions move back to original state (Case 1), another are remained at the position they are migrated (Case 2), and the others migrate nearby defects (Case 3).

XRD analysis: The X-ray diffraction (XRD) patterns were obtained in perovskite QD films using a Rigaku D/max-2500 diffractometer with monochromatized Cu-Kα radiation (λ = 1.5418 Å) at 40 kV and 100 mA.

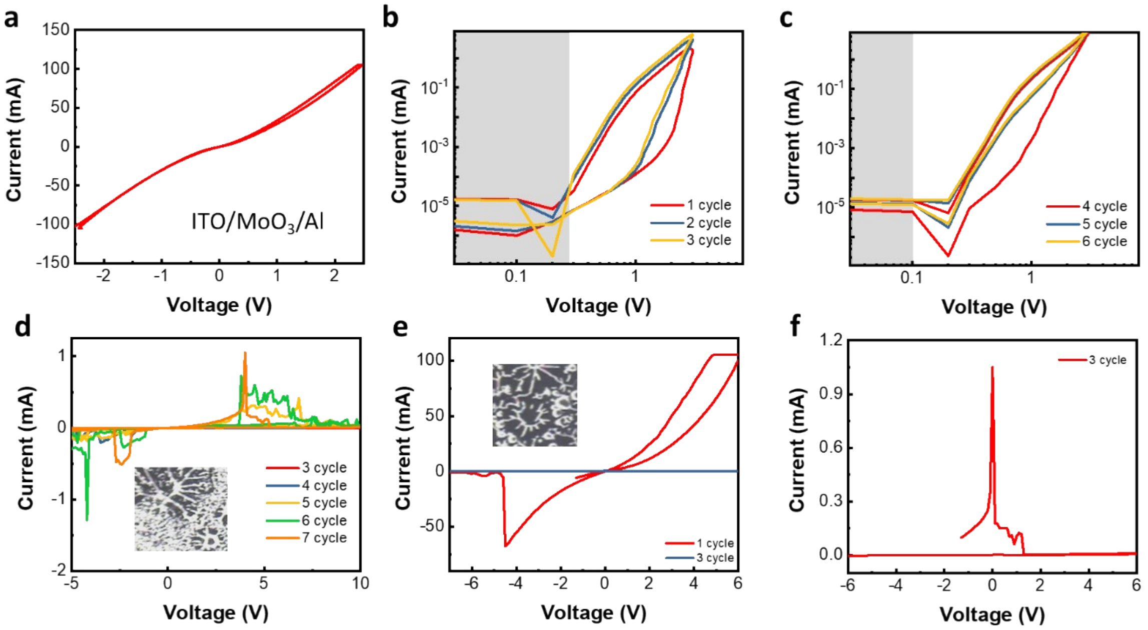

Fig. S1. (a) Current–voltage curve of the capacitor with the ITO/MoO$_3$/Al architecture in –2.5 V to 2.5 V voltage sweep. Current–voltage curves of the capacitor with the ITO/pristine perovskite QD/MoO$_3$/Al architecture in 0 V to 3 V voltage sweeps at log-log scale: (b) 1st – 3rd cycles and (c) 4th– 6th cycles. Current–voltage curves of the capacitor with the ITO/pristine perovskite QD/MoO$_3$/Al architecture (d) in –5 V to 10 V voltage sweeps and (e) –7 V to 6 V voltage sweeps. Inserted images of the capacitors in Fig. S1 d and e were taken after 3rd cycle voltage sweep. (f) Enlarged current–voltage curve of the capacitor with the ITO/pristine perovskite QD/MoO$_3$/Al architecture in –7 V to 6 V voltage sweep at 3rd cycle voltage sweep.

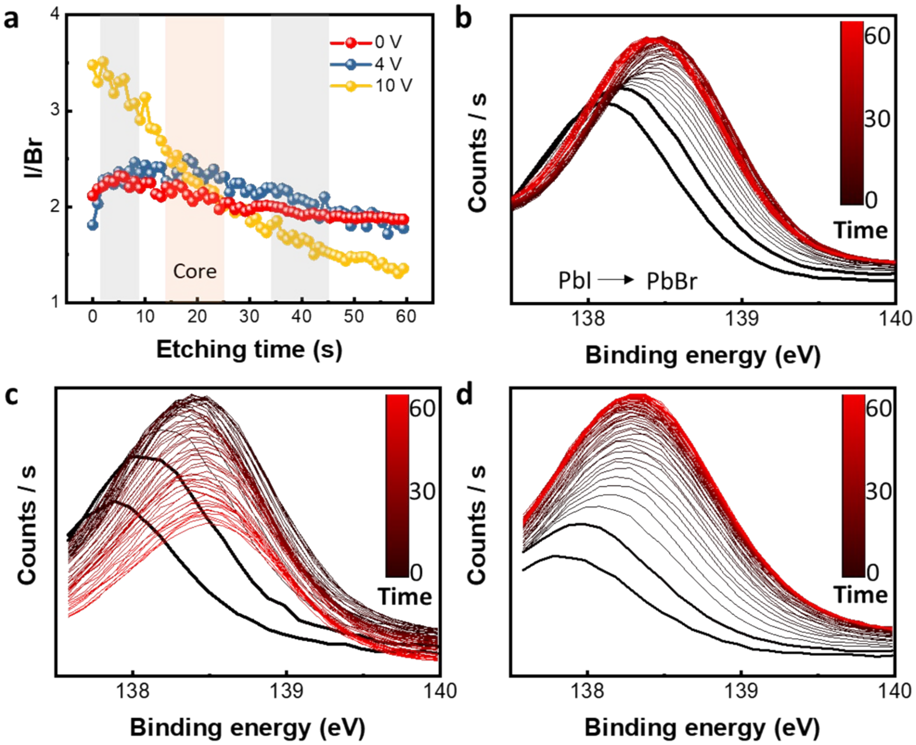

Fig. S2. (a) Depth-profiling XPS of pristine perovskite QDs in the PeLEDs by Ar plasma etching; Changes in I/Br stoichiometry according to depth for pristine perovskite QDs in the PeLEDs after 0 V, 4 V, and 10 V operation for 5 min. Depth-profiling Pb 4f XPS (Pb $4f_{7/2}$) spectrum of (b) pristine perovskite QDs in the PeLED without an electrical field, (c) pristine perovskite QDs in the PeLED operated at 4V for 5 min, and (d) pristine perovskite QDs in the PeLED operated at 10V for 5 min.

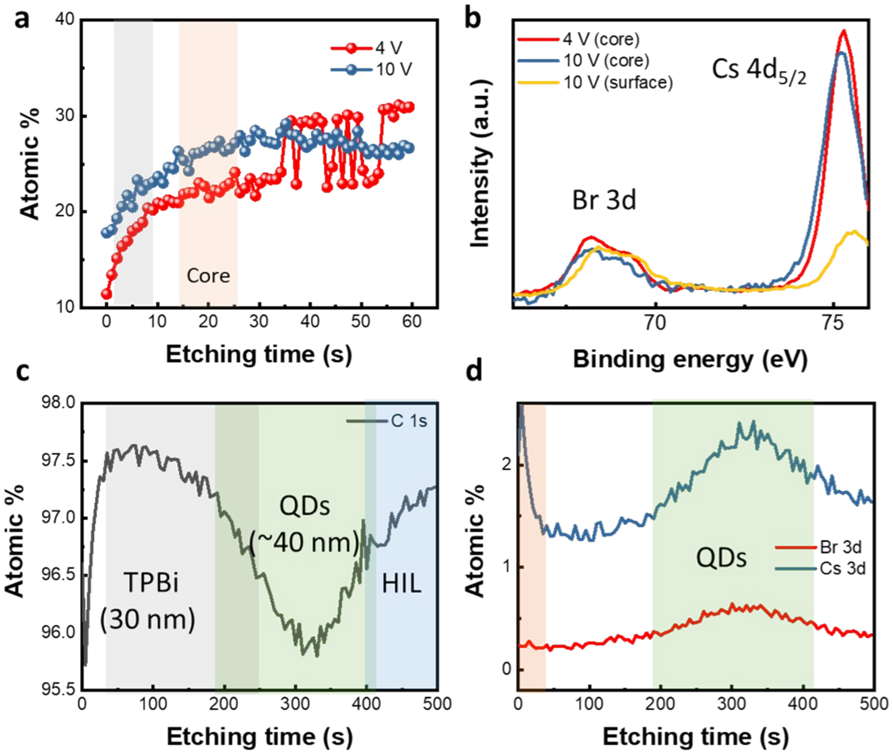

Fig. S3. (a) Depth-profiling XPS of Pb at.% of pristine perovskite QDs in the PeLED operated at 4 V and 10 V for 5 min. (b) XPS spectra of Br 3d and Cs $4d_{5/2}$ in core of pristine perovskite QDs in the PeLED operated at 4 V for 5 min and in core (~18 s Ar plasma-etched) and surface (~2 s Ar plasma-etched) of pristine perovskite QDs in the PeLED operated at 10 V for 5 min. Depth-profiling XPS of (c) C 1s and (d) Cs 3d and Br 3d at.% of pristine perovskite QDs in the PeLED operated at 10 V for 5 min.

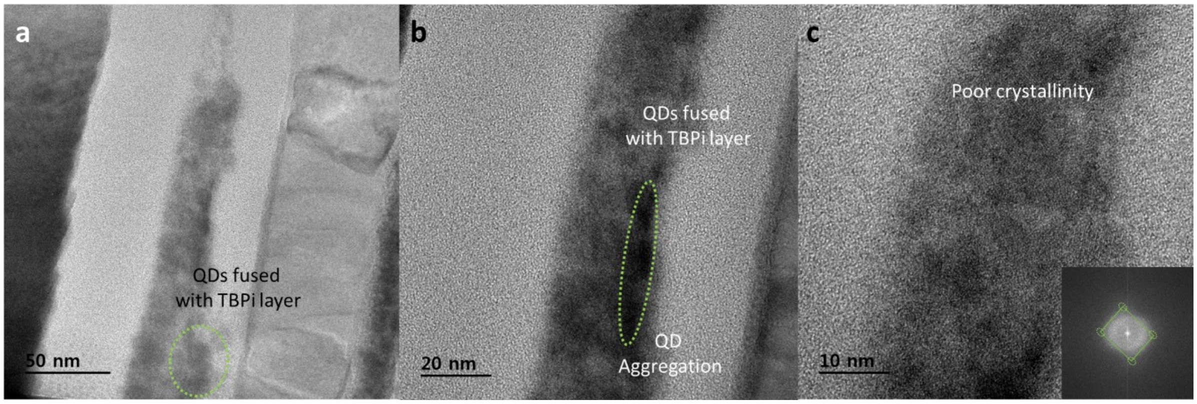

Fig. S4. (a-c) Cross-section TEM images of pristine perovskite QDs in the PeLED operated at 10 V for 5 min. Inset demonstrates FFT pattern at the pristine perovskite QDs in the PeLED nearby TPBi layer.

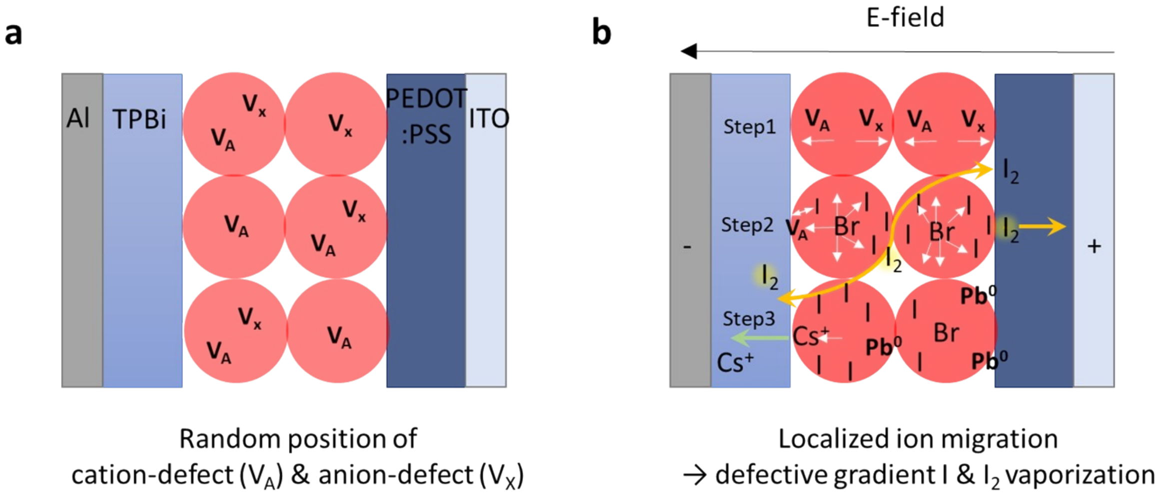

Fig. S5. Schematic of the ion migration in pristine perovskite QDs in the PeLED (a) without an electric field and (b) operated at 10 V for 5 min.

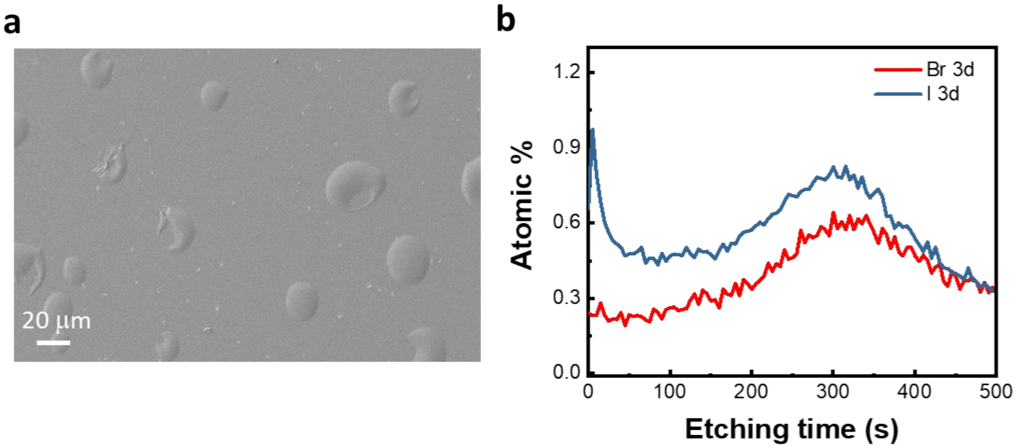

Fig. S6. (a) SEM image of the PeLED (Al side) fabricated using pristine perovskite QDs after operation at 4 V for 5 min. (b) Depth-profiling XPS of I 3d and Br 3d at.% of pristine perovskite QDs in the PeLED operated at 10 V for 5 min.

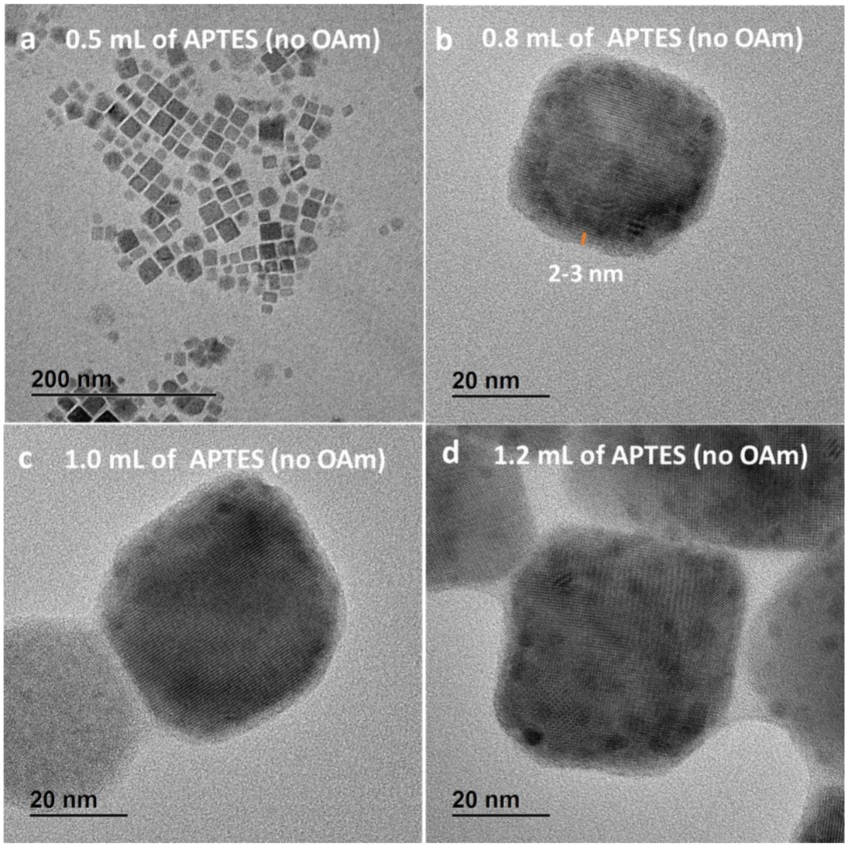

Fig. S7. TEM images of perovskite/SiO_2 core–shell QDs synthesized using (a) 0.5, (b) 0.8, (c) 1.0, (d) 1.2 mL of APTES without OAm.

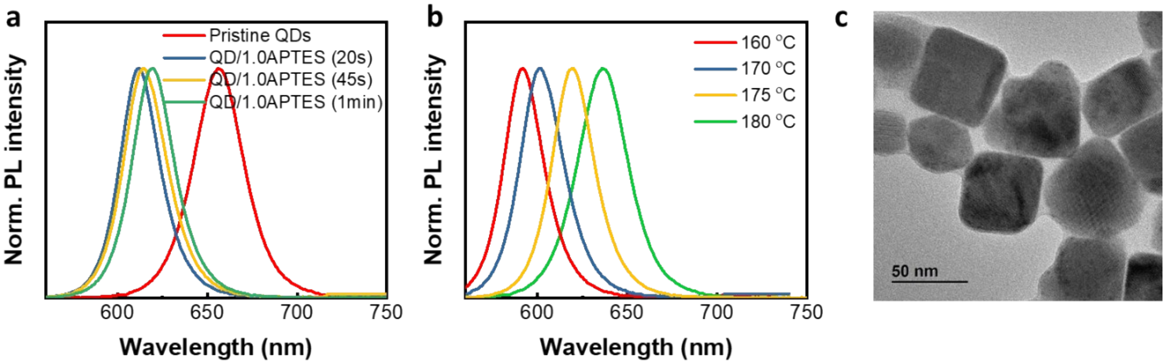

Fig. S8. (a) Solution PL spectra of pristine perovskite QDs and perovskite/SiO_2 core–shell QDs according to reaction time with 1 mL of APTES and 0.4 mL of OAm (temperature: 170 °C). (b) Solution PL spectra of perovskite/SiO_2 core–shell QDs according to reaction temperature with 1 mL of APTES and 0.4 mL of OAm (reaction time: 20 s). (c) TEM image of perovskite/SiO_2 core–shell QDs with 45 s reaction time (1 mL of APTES and 0.4 mL of OAm).

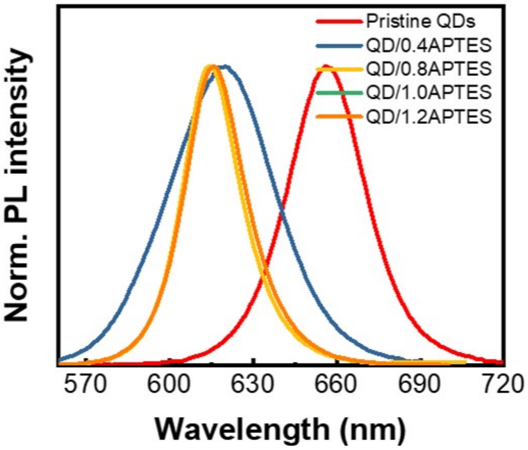

Fig. S9. Solution PL spectra of pristine perovskite QDs and perovskite/SiO_2 core–shell QDs synthesized using different amounts of APTES for obtaining similar λ_{max} values (~615 nm ± 3 nm). (0.4 mL of OAm, reaction time: 20 s, various temperature).

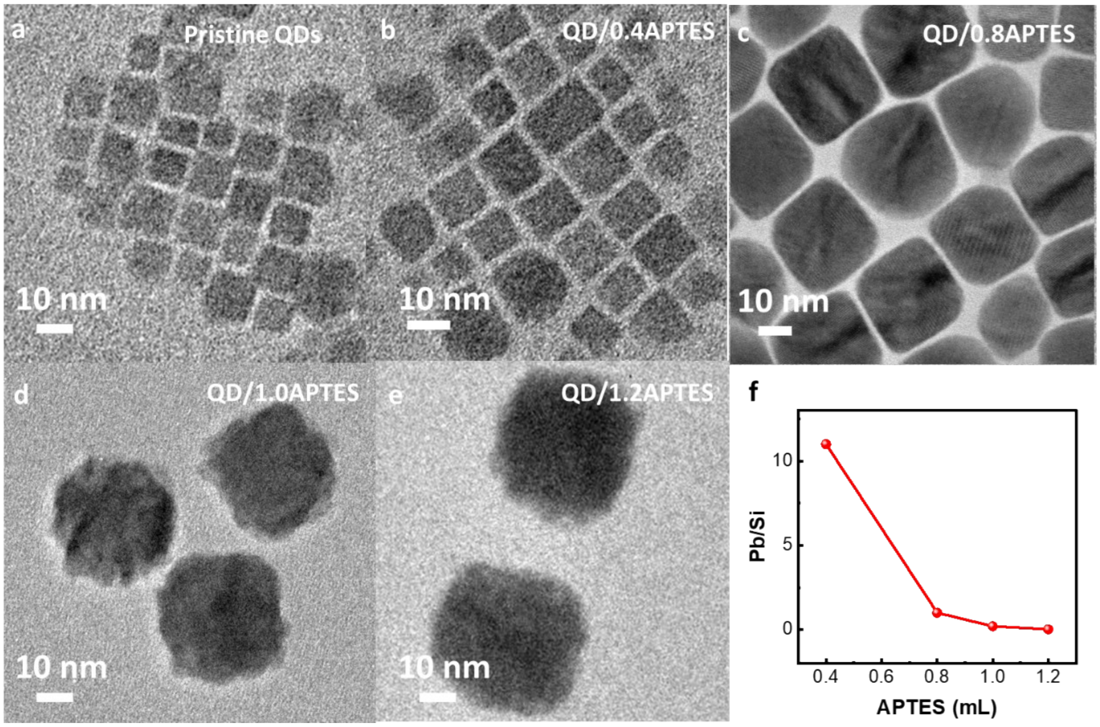

Fig. S10. TEM images of (a) pristine perovskite QDs, (b) QD/0.4APTES, (c) QD/0.8APTES, (d) QD/1.0APTES and (e) QD/1.2APTES (reaction time: 20 s). (f) Pb/Si atomic ratios of perovskite/SiO_2 core–shell QDs using different amounts of APTES and 0.4 mL of OAm.

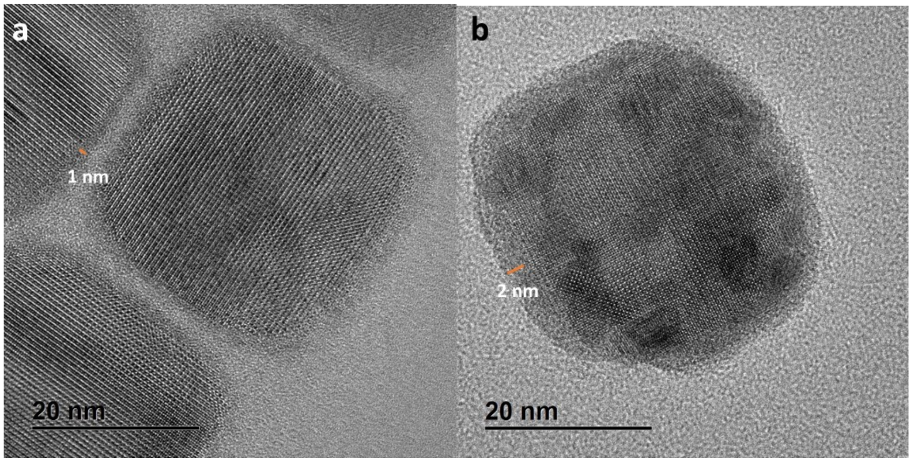

Fig. S11. High-resolution TEM images of (a) QD/0.8APTES and (b) QD/1.0APTES (temperature: 175 °C, reaction time: 20 s, 0.4mL of OAm).

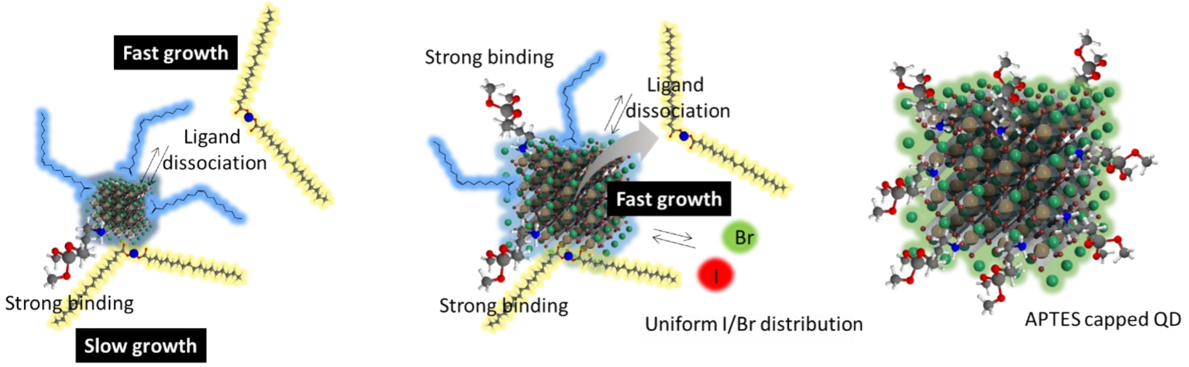

Fig. S12. Crystal growth mechanism of perovskite/SiO$_2$ core–shell QDs without OAm (blue: OAc; yellow: metal-oleate).

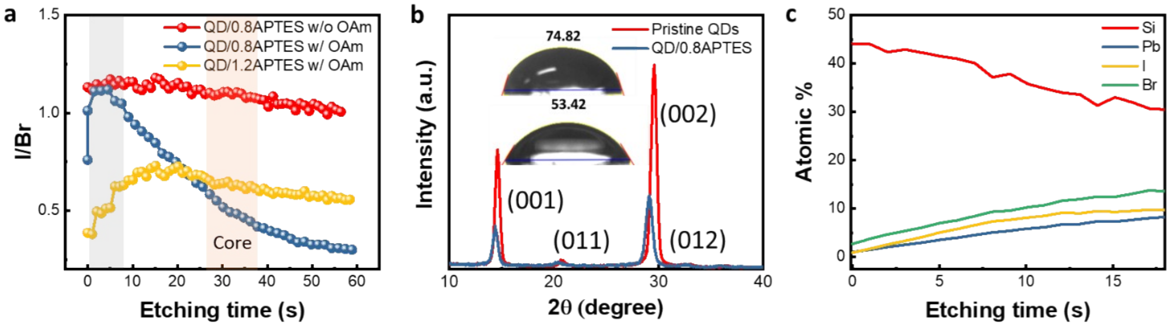

Fig. S13. (a) Depth-profiling XPS of perovskite/SiO$_2$ core–shell QDs by Ar plasma etching; Changes in I/Br stoichiometry according to depth for QD/0.8APTES and QD/1.2APTES. (b) XRD analysis of pristine perovskite QDs and perovskite/SiO$_2$ core–shell QDs; Inset images demonstrate water contact angle of pristine perovskite QDs (~74.82°) and perovskite/SiO$_2$ core–shell QDs (~53.42°). (c) Stoichiometry changes according to depth for QD/1.0APTES.

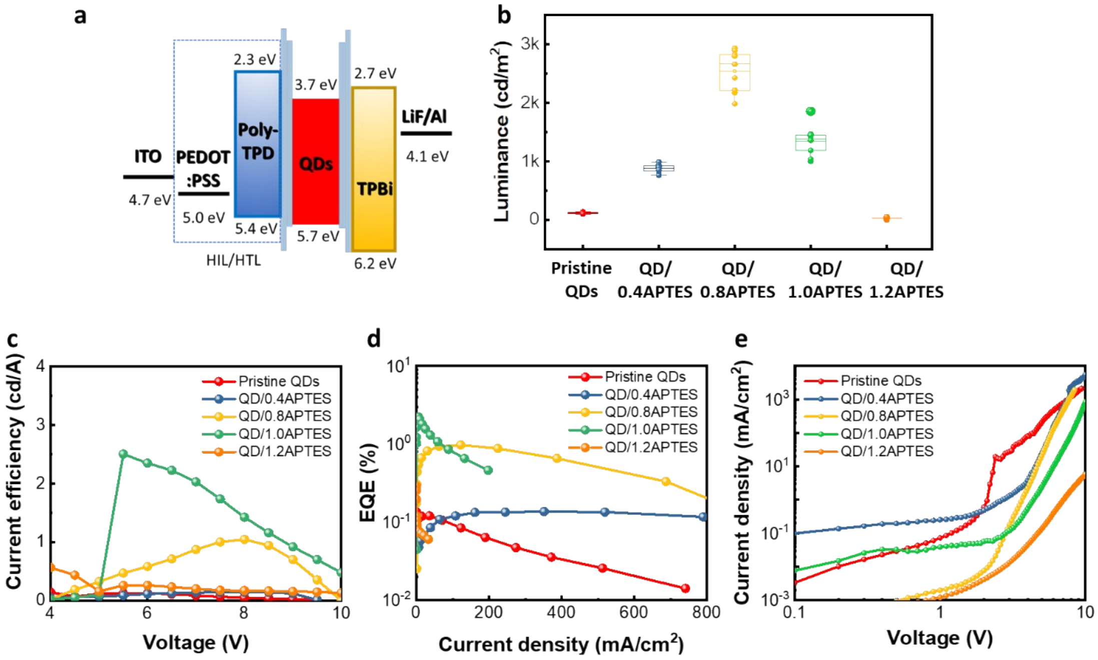

Fig. S14. (a) Energy level diagram of materials and device architectures used in this work. (b) Statistical analysis on the luminances of PeLEDs fabricated using pristine perovskite QDs, QD/0.4APTES, QD/0.8APTES, QD/1.0APTES, and QD/1.2APTES (whiskers plot). (c) Current efficiencies *vs.* voltages and (d) EQEs *vs.* current densities curves of PeLEDs fabricated using pristine perovskite QDs, QD/0.4APTES, QD/0.8APTES, QD/1.0APTES, and QD/1.2APTES. (e) HODs fabricated using pristine perovskite QDs, QD/0.4APTES, QD/0.8APTES, QD/1.0APTES, and QD/1.2APTES.

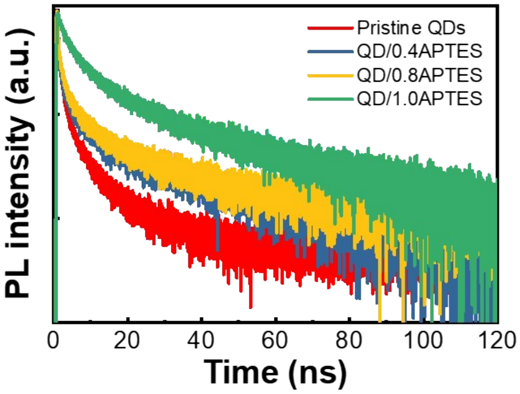

Fig. S15. PL decay profiles of pristine perovskite QDs, QD/0.4APTES, QD/0.8APTES, and QD/1.0APTES films at log scale.

Table S1. PL lifetimes of pristine perovskite QDs and perovskite/SiO_2 core–shell QDs.

Sample	τ_1/ns (f_1)	τ_2/ns (f_2)	τ_3/ns (f_3)	χ^2	τ_{avr}/ns
Pristine QDs	2.39 (0.21)	0.37 (0.75)	12.9 (0.04)	1.051	1.30
QD/0.4 APTES	3.77 (0.27)	0.42 (0.65)	47.6 (0.08)	1.050	5.10
QD/0.8 APTES	3.82 (0.28)	0.40 (0.64)	25.53 (0.08)	1.084	3.37
QD/1.0 APTES	10.14 (0.36)	2.25 (0.51)	57.07 (0.13)	0.961	12.22

Monitored wavelength was λ_{max} of each perovskite QDs: 648 nm for pristine perovskite QDs, 615 nm for perovskite/SiO_2 core—shell QDs. PL decay curves were fitted by a three-exponential function to investigate the exciton dynamics of perovskite QD films. The intensity-weighted average exciton lifetime (τ_{avr}) was $f_1\tau_1 + f_2\tau_2 + f_3\tau_3$, where f_1, f_2 and f_3 are fractional intensities and τ_1, τ_2 and τ_3 are lifetimes. χ^2 is the reduced chi-squared value.

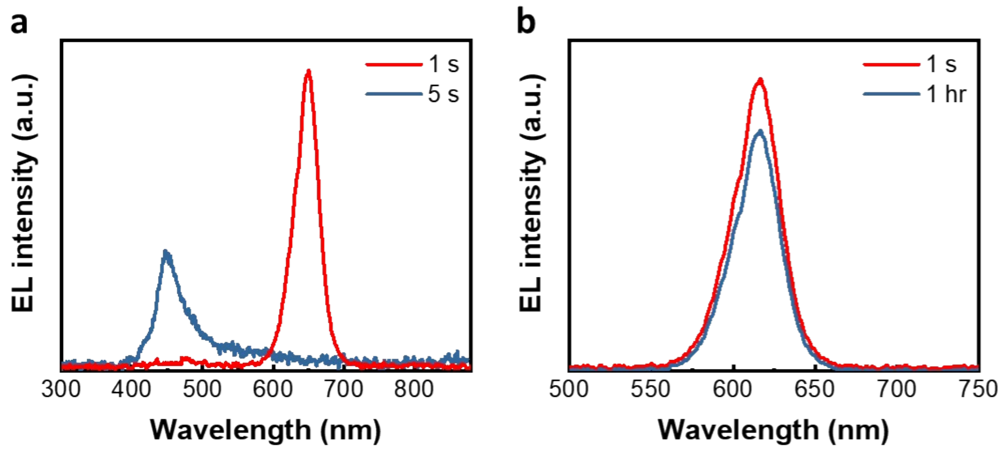

Fig. S16. (a) EL spectra of pristine perovskite QD-based PeLED operated at 6 V (~1 s and 5 s). (b) EL spectra of QD/0.8APTES-based PeLED operated at 6 V (~1 s and 1 hr).

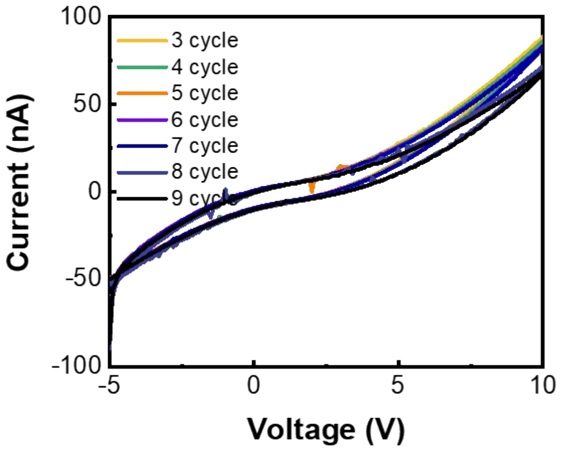

Fig. S17. Current–voltage curves of the capacitor with the ITO/0.8APTES (60 nm)/MoO_3/Al architecture in –5 V to 10 V voltage sweeps.

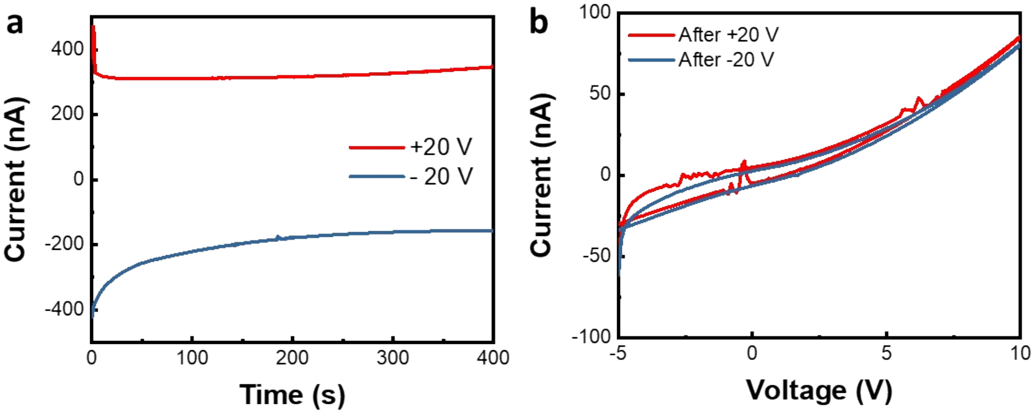

Fig. S18. (a) Current *vs.* time characteristics of the capacitor with the ITO/0.8APTES (60 nm)/MoO_3/Al architecture in continuous +20 to −20 V operation. (b) Current–voltage curves of the capacitor with the ITO/0.8APTES (60 nm)/MoO_3/Al architecture after +20 and −20 V operation (operation time: 400 s).

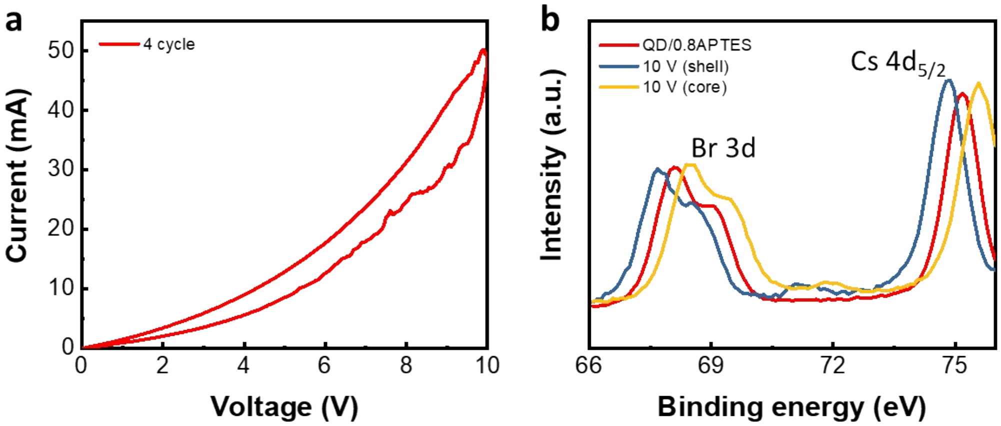

Fig. S19. (a) Current–voltage curve of the capacitor with the ITO/0.8APTES (30 nm)/MoO_3/Al architecture during 4th cycle sweep (0 to 10 V). (b) XPS spectra of Br 3d and Cs $4d_{5/2}$ in core of QD/0.8APTES without an electric field and in core and shell of QD/0.8APTES in the PeLED operated at 10 V for 5 min.

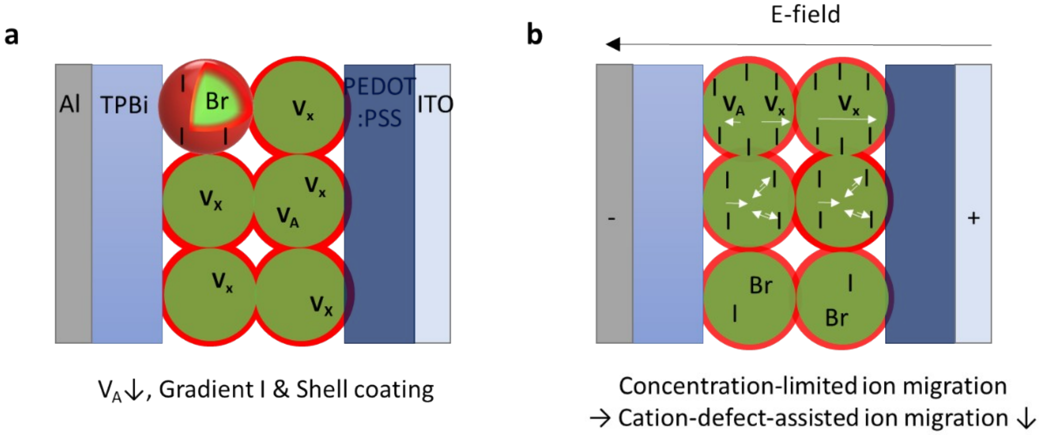

Fig. S20. Schematic of the ion migration in QD/0.8APTES in the PeLED (a) without an electric field and (b) operated at 10 V for 5 min.

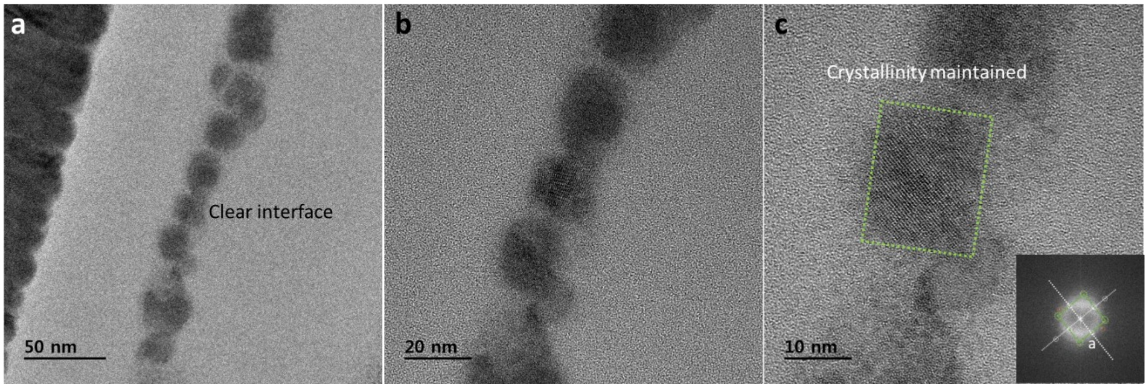

Fig. S21. (a-c) Cross-section TEM image of QD/0.8APTES in the PeLED operated at 10 V for 5 min. Inset demonstrates FFT pattern at the QD/0.8APTES in the PeLED nearby TPBi layer.

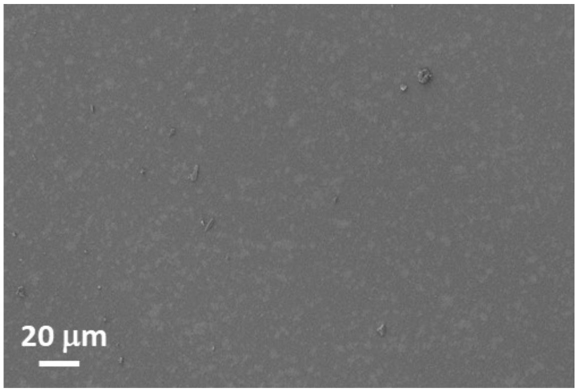

Fig. S22. SEM image of the PeLED (Al side) fabricated using QD/0.8APTES after operation at 10 V for 5 min.

II. Optical and perovskite QD structure characterization

Optical properties of perovskite QDs: The absorption spectra of perovskite QDs are measured using the UV-Vis spectrometer (JASCO V-650 spectrophotometer). Steady-state photoluminescence (PL) spectra are obtained using two monochromator (SP-2150i and SP-2300i, Acton) systems equipped with a photomultiplier tube (PMT, Acton PD 471) and a Xenon lamp as an excitation light source. The PLQYs of perovskite QD solutions are obtained relative to a Rhodamine B (PLQY = ∼70% in ethanol). PL decays of perovskite QD films are investigated using time-correlated single photon counting (TCSPC) measurements. A pulsed diode-laser head (LDH-P-C-405, PicoQuant) coupled with a laser-diode driver (PDL 800-B, PicoQuant) is used as the excitation source with a repetition rate of 5 MHz. The excitation wavelength is 400 nm. The PL is spectrally resolved using collection optics and a monochromator (SP-2150i, Acton). A TCSPC module (PicoHarp 300, PicoQuant) with a MCP-PMT (Hamamatsu, R3809U-59) is used for ultrafast detection. The total instrument response function (IRF) is less than ~140 ps, and the temporal resolution is ~ 8 ps. Deconvolution of PL decay curves, which separates the IRF and actual PL decay signal, is performed using fitting software (FluoFit, PicoQuant) to deduce the time constant associated with each exponential decay curve.

Surface Tension: The surface tensions of perovskite QD films are measured using contact angle measurements (First Ten Angstroms FTA1000B) where drop shape analysis is used to calculate the surface tension from the shadow image of a water drop.

Transmission Electron Microscopy: Transmission electron microscopy (Tecnai G2 F30 S-Twin 300 kV) is used to define the lattice parameter of perovskite QDs. Samples for cross-section TEM were prepared by FIB-SEM (Crossbeam550, ZEISS) and cross-section TEM was measured by (Tecnai G2 F30 S-Twin 300 kV). PeLEDs for cross-section TEM measurements are fabricated following method. The PeLEDs are fabricated on bare ITO coated glass (~20 Ω/sq). The PEDOT: PSS (AI 4083) is spin-coated on the ITO substrate, after 60 s O_2 plasma treatment, used as a hole injection layer (HIL). The PEDOT: PSS (50 nm) coated ITO substrate is baked at 150 °C for 30 min in air. After then, the perovskite QDs is spin-coated: ~40 nm for pristine perovskite QDs and ~25-30 nm for perovskite/SiO_2 core–shell QDs. After then, TPBi (30 nm)/Al (150 nm) is deposited on the top of perovskite QDs layer as an electron transporting layer (ETL) and a cathode electrode in a high-vacuum chamber (base pressure of $\sim 3 \times 10^{-7}$ torr) by using thermal evaporation.

III. Device preparation and electrical properties characterization

PeLEDs fabricated using pristine perovskite QDs: The solution processed PeLEDs are fabricated on bare ITO coated glass. The conductivity of anode is around 20 Ω/sq. The PEDOT: PSS (AI 4083) is spin-coated on the ITO substrate, after 60 s O_2 plasma treatment, used as a hole injection layer (HIL). The PEDOT: PSS (50 nm) coated ITO substrate is baked at 150 °C for 30 min in air. Next, Poly-TPD (30 nm) in chlorobenzene (8 mg/mL) is spin-coated and basked at 150 °C for 30 min. After then, the pristine perovskite QDs (40 nm) is spin-coated. After then, TPBi (30 nm)/LiF (1 nm)/Al (150 nm) is deposited on the top of perovskite QD layer as an electron transporting layer (ETL) and a cathode electrode in a high-vacuum chamber (base pressure of $\sim 3 \times 10^{-7}$ torr) by using thermal evaporation.

PeLEDs fabricated using perovskite/SiO_2 core–shell QDs: The solution processed PeLEDs are fabricated on bare ITO coated glass. The conductivity of anode is around 20 Ω/sq. The PEDOT: PSS (50 nm) coated ITO substrate is baked at 150 °C for 30 min in air. After then, the perovskite/SiO_2 core–shell QDs (25-30 nm) is spin-coated. After then, TPBi (30 nm)/LiF (1 nm)/Al (150 nm) is deposited on the top of perovskite/SiO_2 core–shell QD layer as an electron transporting layer (ETL) and a cathode electrode in a high-vacuum chamber (base pressure of $\sim 3 \times 10^{-7}$ torr) by using thermal evaporation.

PeLEDs characterizations: Current density–voltage–luminance (J–V–L) characteristics of PeLEDs are measured with a Keithley 2400 source meter and luminance meter (CS-2000, Minolta). The EL spectra of PeLEDs are obtained using a K-mac SV2100 spectrometer.

HOD fabrication: HODs are fabricated on bare ITO coated glass. The conductivity of anode is around 20 Ω/sq. The PEDOT:PSS is spin-coated on the ITO substrate, after 60 s O_2 plasma treatment, used as a hole injection layer (HIL). The PEDOT:PSS (50 nm) coated ITO substrate is baked at 150 °C for 30 min in air. After then, the perovskite QDs is spin-coated. After then, MoO_3 (10 nm)/Ag (150 nm) is deposited on the top of perovskite QDs layer as a cathode electrode in a high-vacuum chamber (base pressure of $\sim 3 \times 10^{-7}$ torr) by using thermal evaporation. The hole mobility is calculated by space-charge-limited current (SCLC) in the commonly used Mott-Gurney equation[1]; $J = (9\varepsilon\mu V^2)/(8d^3)$.

Reference

1. L. Qian, Y. Zheng, J. Xue and P. H. Holloway, *Nat. Photonics*, 2011, **5**, 543-548.